BJP British Journal of Pharmacology

DOI:10.1111/bph.12443
www.brjpharmacol.org

Themed Section: The pharmacology of TRP channels

RESEARCH PAPER

Naringenin inhibits the growth of *Dictyostelium* and MDCK-derived cysts in a TRPP2 (polycystin-2)-dependent manner

A Waheed[1], M H R Ludtmann[2], N Pakes[2], S Robery[2], A Kuspa[3], C Dinh[3], D Baines[4]*, R S B Williams[2*†] and M A Carew[1*†]

[1]*School of Pharmacy & Chemistry, Kingston University, Kingston upon Thames, Surrey, UK,* [2]*Centre for Biomedical Science, School of Biological Sciences, Royal Holloway University of London, Egham, Surrey, UK,* [3]*Department of Biochemistry and Molecular Biology, Baylor College of Medicine, Houston, TX, USA, and* [4]*Biomedical Sciences, St George's University of London, London, UK*

Correspondence
Dr Mark A Carew, School of Pharmacy & Chemistry, Kingston University, Penrhyn Road, Kingston upon Thames, Surrey KT1 2EE, UK. E-mail: m.carew@kingston.ac.uk
Prof Robin SB Williams, Centre for Biomedical Sciences, School of Biological Sciences, Royal Holloway TW20 0EX UK. E-mail: robin.williams@rhul.ac.uk

*Joint last author.
†Joint corresponding author.

Keywords
polycystic kidney disease; polycystin-2; naringenin; *Dictyostelium*; polyphenol; cell growth

Received
5 March 2013
Revised
4 September 2013
Accepted
13 September 2013

BACKGROUND AND PURPOSE
Identifying and characterizing potential new therapeutic agents to target cell proliferation may provide improved treatments for neoplastic disorders such as cancer and polycystic diseases.

EXPERIMENTAL APPROACH
We used the simple, tractable biomedical model *Dictyostelium* to investigate the molecular mechanism of naringenin, a dietary flavonoid with antiproliferative and chemopreventive actions *in vitro* and in animal models of carcinogenesis. We then translated these results to a mammalian kidney model, Madin-Darby canine kidney (MDCK) tubule cells, grown in culture and as cysts in a collagen matrix.

KEY RESULTS
Naringenin inhibited *Dictyostelium* growth, but not development. Screening of a library of random gene knockout mutants identified a mutant lacking TRPP2 (polycystin-2) that was resistant to the effect of naringenin on growth and random cell movement. TRPP2 is a divalent transient receptor potential cation channel, where mutations in the protein give rise to type 2 autosomal dominant polycystic kidney disease (ADPKD). Naringenin inhibited MDCK cell growth and inhibited cyst growth. Knockdown of TRPP2 levels by siRNA in this model conferred partial resistance to naringenin such that cysts treated with 3 and 10 μM naringenin were larger following TRPP2 knockdown compared with controls. Naringenin did not affect chloride secretion.

CONCLUSIONS AND IMPLICATIONS
The action of naringenin on cell growth in the phylogenetically diverse systems of *Dictyostelium* and mammalian kidney cells, suggests a conserved effect mediated by TRPP2 (polycystin-2). Further studies will investigate naringenin as a potential new therapeutic agent in ADPKD.

LINKED ARTICLES
This article is part of a themed section on the pharmacology of TRP channels. To view the other articles in this section visit http://dx.doi.org/10.1111/bph.2014.171.issue-10

Abbreviations
ADPKD, autosomal dominant polycystic kidney disease; PKD, polycystic kidney disease; PKD1, the gene-encoding TRPP1 in humans; *pkd1*, the gene-encoding TRPP1 in Dictyostelium; PKD2, the gene-encoding TRPP2 in humans; *pkd2*, the gene-encoding TRPP2 in Dictyostelium; *pkd2*$^{-}$, the *Dictyostelium* mutant lacking the *pkd2* gene

Introduction

The development of new treatments for a disease requires knowledge of the molecular target(s) of those treatments. The social amoeba, *Dictyostelium discoideum*, is a simple biomedical model commonly used to study developmental and cellular biology. *Dictyostelium* has recently been used in early drug development studies (Chang *et al.*, 2012) and to identify molecular pathways regulating drug action (Terbach *et al.*, 2011). In its natural forest-floor habitat, *Dictyostelium* exists in its amoeboid state and feeds on bacterial cells by phagocytosis (Williams *et al.*, 2006). When nutrients are scarce, cells aggregate to form fruiting bodies containing spores that are dormant and resistant to desiccation. Growth and development are controlled by a range of separate signalling pathways that can be probed at the molecular level by screening libraries of insertional mutants, constructed by restriction enzyme-mediated integration (REMI). This approach has provided new insights into how current therapeutic agents regulate cellular function (Williams *et al.*, 2006), for example, in identifying common signalling pathways targeted by lithium and valproic acid in the treatment of bipolar disorder, and is increasingly being used to identify cellular mechanisms controlling drug targets using growth and development (Terbach *et al.*, 2011) or cell movement (Robery *et al.*, 2011) as phenotypic readouts.

Naringenin (4′,5,7-trihydroxyflavanone; Figure 1) is a member of the flavonone subclass of flavonoids, a large family of plant polyphenols. Naringenin is ingested mostly as naringin (its glycoside) and is available at relatively high doses (~30 mg naringin 100 mL^{-1}) in grapefruit juice (http://www.phenol-explorer.eu). Naringenin is bioavailable after reasonable doses; for example, a dose of 139–265 mg naringenin yielded 0.7–14.8 μM of the aglycone in the blood after absorption (Erlund *et al.*, 2001). After phase 2 metabolism, naringenin glucuronides and sulphates are detected in low micromolar concentrations (Manach *et al.*, 2005). In common with many flavonoids, naringenin inhibits growth in tumour cells by a number of mechanisms, including cell cycle arrest and p53-dependent apoptosis (Meiyanto *et al.*, 2012). Naringenin also suppresses colon cancer in rats (Leonardi *et al.*, 2010) and inhibits metastasis and tissue invasion (Weng and Yen, 2012). The chemopreventive actions of naringenin may include activation of certain cytochrome P450 isozymes and phase 2 enzymes involved in the detoxification of potential carcinogens (Moon *et al.*, 2006; Kale *et al.*, 2008).

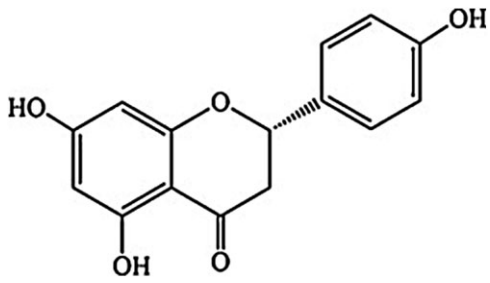

Figure 1
Structure of naringenin (4′,5,7-trihydroxyflavanone).

Since a previous study had shown that naringenin blocked *Dictyostelium* cell growth (Russ *et al.*, 2006), we sought to identify the molecular mechanism of naringenin function in this model. By screening a library of *Dictyostelium* REMI mutants, it was possible to identify genes conferring resistance to naringenin. We then used the appropriate mammalian system to study the role of the identified gene product in mediating the actions of naringenin on cell growth. Our data have identified a new candidate for naringenin-mediated cell function: polycystin-2 (TRPP2), a Ca^{2+} permeable non-selective cation channel implicated in the development of autosomal dominant polycystic kidney disease (ADPKD; González-Perrett *et al.*, 2001; Vassilev *et al.*, 2001). In this disease, kidney cysts develop due to a defect in proliferation and because of fluid secretion into the cysts (Terryn *et al.*, 2011). About 85% of ADPKD cases result from mutations in the TRPP1 (polycystic kidney disease-1) gene and protein, with the remainder accounted for by mutations in the TRPP2 (PKD2) gene and protein (Chapin and Caplan, 2010). We therefore followed up on our own initial observations in *Dictyostelium* by studying the involvement of TRPP2 in the effects of naringenin on the growth of Madin-Darby canine kidney (MDCK) cells and cysts. We found that TRPP2 (polycystin-2) mediated the growth-inhibitory effects of naringenin in both systems.

Methods

Dictyostelium *growth assays*

Dictyostelium discoideum wild-type cells (Ax2) were grown in shaking suspension in Axenic medium (ForMedium Co. Ltd, Norfolk, UK) at 120 rpm (21°C) and harvested in mid-log phase (4×10^6). Cells (1×10^6 cells·mL^{-1}) were then resuspended in Axenic medium containing 100 μM naringenin or DMSO and counted at 24 h intervals.

Dictyostelium *insertional mutagenesis library screening*

Dictyostelium wild-type cells (Ax4) were mutagenized by REMI of plasmid DNA using pBBC plasmids, which are derivatives of the pBSR1 plasmid (Adachi *et al.*, 1994) that contain 60mer DNA barcodes (C. Dinh, pers. comm.). REMI was performed using three combinations of restriction enzymes for plasmid linearization/electroporation (BamHI/DpnII, EcoRI/ApoII and SphI/NlaIII). Clonal transformants were propagated in 24-well culture plates and stored at –80°C in 10% DMSO for future recovery. The residual cells from these plates were spotted on a bacterial growth plate, allowed to grow for 2 days, and collected as pools (24 mutants per pool). A number of these pools of 24 (28–32 pools) were combined into 30 large pools of 672–768 mutants. Twenty-five large pools were used in the enrichment experiments that were carried out for each pool, in triplicate, in 10 cm Petri dishes with 10 mL of HL-5 supplemented with 100 μg·mL^{-1} streptomycin and 100 U·mL^{-1} penicillin (Sussman, 1987). Naringenin (200 μM final concentration) was added to 5×10^6 mutant cells in 10 mL of supplemented HL-5. After 3 days or when cell concentration reached ~2×10^6 cells·mL^{-1}, 1 mL of the initial culture media was removed and added to 9 mL of fresh media containing

naringenin. The same procedure was repeated for 21 days. Genomic DNA was purified from cells that were collected from each culture dish and plasmid insertion sites were cloned as described previously (Kuspa, 2006). After a mutant's insertion site was identified by plasmid rescue, a clonal strain was recovered from the 24-well frozen stock to confirm resistance to growth inhibition by naringenin and for further analysis.

Dictyostelium pkd2$^-$ *recapitulation*

Knockout constructs were created using methods described previously (Pakes *et al.*, 2012). Briefly, 5′ and 3′ fragments flanking the *Dictyostelium pkd2* was amplified by PCR (peqSTAR 96 Universal Gradient, Erlangen, Germany) from wild-type genomic DNA. The 5′ terminal targeting fragment was amplified using AAGGGATCCAATACCTTGAAATTAA TAATCCATC and TTAACTGCAGCTGATGCTGTC, and the 3′ terminal fragment was amplified using CTGATATTGCCT CATTCCATGGCTTCG and TTGGTGATTGTGGGGTACCAG TAC. The 5′ and 3′ PCR fragments were cloned into the plPBLP expression vector using BamHI/PstI (5′ fragment-500 bp) and NcoI/KpnI (3′ fragment-744 bp) restriction sites, respectively, incorporating the gene in the reverse orientation to the blasticidin resistance cassette. The knockout cassette was linearized and transformed into wild-type cells via electroporation (Gene Pulser Xcell, Bio-Rad, Hertfordshire, UK). Positive transformants were selected in nutrient media containing blasticidin (10 μg·mL^{-1}). Independent clones were screened for homologous integration by PCR, using diagnostic PCR products for the presence of target gene genomic DNA and knockout vector sequences, as well as a diagnostic PCR product only found for homologous intergrant for both N and C-terminal regions of the knockout cassette. Triplicate independent isolates were identified, clonally plated onto *Raoultella planticola*, and isogenic colonies were used in subsequent experiments.

Dictyostelium *random cell movement assay*

To analyse the effect of naringenin on *Dictyostelium* random cell movement, wild-type and *pkd2*$^-$ cells were grown in shaking suspension in Axenic medium for 48 h, washed and resuspended in phosphate buffer at 1.7×10^6 cells·mL^{-1}, and treated with 30 nM cAMP at 6 min intervals while shaking at 120 rpm as described previously (Robery *et al.*, 2011). Cells were then shaken in the presence of 200 μM naringenin or 0.7% DMSO (solvent control) for 1 h, transferred into 8-well glass coverslips (Thermo Fisher, Loughborough, UK) and random cell movement was recorded by capturing one image every 15 s for 5 min. A minimum of three independent experiments were performed for each cell and condition, whereby an average ~10 cells were quantified per experiment. Random cell movement was analysed using the Quimp 11b software package for ImageJ (Tyson *et al.*, 2010). Data were imported into MATLAB where changes in motility, circularity, distance travelled and number of protrusions formed were monitored for each cell line in the presence and absence naringenin. The effect of naringenin was assessed in relation to distance travelled by cells during random cell movement, cell circularity, number of protrusions and motility. Data were compared using one-way ANOVA with Tukey's *post hoc* test.

MDCK cell culture

MDCK C7 cells were a generous gift from Dr Anselm Zdebik (Department of Neuroscience, Physiology & Pharmacology, University College London). MDCK cells were cultured in DMEM (Life Technologies, Ltd., Paisley, UK) containing 10% (v v^{-1}) FBS, gentamycin (40 μg·mL^{-1}), penicillin (100 units·mL^{-1}) and streptomycin (1040 μg·mL^{-1}), and were maintained at 37°C in a humidified, 5% CO_2 atmosphere. Cells of less than 18 passage numbers were used for all cytotoxicity and cyst growth studies.

MDCK cell viability assays

Naringenin was dissolved in DMSO (to a maximum of 0.1% DMSO v v^{-1}) and evaluated for its antiproliferative effect on MDCK cells using the sulforhodamine B (SRB) assay. Cells were seeded in complete DMEM in a 96-well plate (10 000 cells per well), allowed to adhere for 24 h then incubated with naringenin (1–100 μM) for 24–48 h. The medium was removed and 100 μL of SRB solution [0.4% (w/v) in 1% acetic acid] was added to each well and plates were incubated for 10 min at room temperature. The SRB solution was removed and cells were washed five times with 1% acetic acid (200 μL per well) before air drying. SRB bound to adherent cells was solubilized with 10 mM Tris base (unbuffered) and plates were placed on a horizontal shaker for at least 10 min at room temperature. Absorbance was read at 550 nm using an ELx808 Absorbance Microplate reader (Biotek, Potton, UK). Actinomycin-D (5 μM) was used as a positive control. The neutral red assay was performed as described previously (Repetto *et al.*, 2008) with readings at 510 nm. EC_{50} values were calculated by four-parameter non-linear regression using GraphPad Prism (GraphPad Software, San Diego, CA, USA).

MDCK cyst culture and measurement

For cyst growth studies, we followed a published protocol (Li *et al.*, 2004). In brief, MDCK cells were cultured in 24-well plates. A cell suspension (~800 cells per well) was mixed with 0.4 mL ice-cold collagen (PureCol, Nutacon BV, Leimuiden, The Netherlands) supplemented with DMEM containing 10% (v/v) FBS, gentamycin (40 μg·mL^{-1}), penicillin (100 units·mL^{-1}), streptomycin (1040 μg·mL^{-1}), 10 mM HEPES and 27 mM $NaHCO_3$. Plates containing cells in collagen were incubated at 37°C in a humidified, 5% CO_2 atmosphere for about 2 h until the collagen sets. DMEM (1.5 mL) containing 10% FBS and forskolin (10 μM; Tocris Biosciences, Bristol, UK) was added to each well and plates were placed back in the incubator. Cells were replenished with fresh DMEM medium supplemented with forskolin (10 μM) after every 2 days until the end of day 12. Cells transformed into cysts within 3 days of plating and were photographed using an inverted microscope (Leica, Milton Keynes, UK) at ×100 magnification. On day 6, a total of 50 cysts each with a diameter >50 μm were selected and referenced using microscope slide-grids underneath each well. The same protocol was followed for the transfected MDCK cells. To evaluate the potential effect on cyst growth, naringenin (in a maximum of 0.1% DMSO) at 1, 3, 10, 30, 60, 100 μM, or metformin (10 μM; Sigma Aldrich, Poole, UK), or vehicle control (0.1% DMSO) were added in DMEM (1.5 mL per well) containing

forskolin (10 μM) on days 6, 8 and 10. Photographs of referenced cysts were taken on days 6, 8, 10 and 12. Cyst area (mm^2) was measured using Image J software (v 1.4; Schneider *et al.*, 2012).

Electrophysiological measurements of MDCK monolayers

MDCK cells were seeded onto Snapwell permeable supports (0.4 μm pore, polyester membrane, 12 mm diameter, Costar 3801; Corning Inc, Corning, NY, USA) at 2×10^5 cells·cm^{-2}. Cells formed monolayers in culture in a humidified incubator (37°C, 5% CO_2). Culture medium was replaced every 2 days and monolayers were used in experiments after 12–13 days in culture. Monolayers were mounted in Ussing chambers and bathed both sides with Krebs-Henseleit (KH) buffer: in mM, NaCl 117, $NaHCO_3$ 25, KCl 4.7, $MgSO_4$ 1.2, KH_2PO_4 1.2, glucose 11, $CaCl_2$ 2.5, bubbled with 95% O_2/5% CO_2 to maintain pH at 7.45. Experiments were performed at 37°C using heated water-jacketed buffer reservoirs. The transepithelial potential difference (Vt) generated across MDCK monolayers was clamped to 0 mV and the short-circuit current (I_{SC}) recorded using a DVC-1000 voltage-clamp amplifier (World Precision Instruments, New Haven, CT, USA) via an analog–digital convertor (Bio-Pac MP100) and Acknowledge 3.8.2 software (Bio Pac Systems Inc., Goleta, CA, USA). Brief (2 s) voltage steps from 0 to 1 mV were applied periodically and the change in current used to calculate transepithelial resistance. MDCK monolayers had a spontaneous Vt of –4.7 ± 1.3 mV on mounting, baseline I_{SC} was 1.0 ± 0.3 μA·cm^{-2} and transepithelial resistance was 2152 ± 308 Ωcm^2 (n = 12).

siRNA TRPP2 transfection

MDCK cells were grown until 80% confluent. For transfection experiments, cells were incubated overnight in reduced serum medium Opti-MEM (31985; Life Technologies, Ltd.) prior to transfection. Cells were then transfected with 20 nM (final concentration per well) canine TRPP2 siRNA or scrambled control siRNA (Ambion Cy3-labeled siRNA; Invitrogen) in a lipid-based transfection reagent lipofectamine 2000 (Invitrogen) at 1:1000 dilution for 24 h. Cells were allowed to recover in DMEM without antibiotics for 12 h. The following day, cells were re-transfected using a similar procedure. This double transfection procedure resulted in a transfection efficiency of approximately 60–70%. Following transfection, cells were grown for 24–48 h for Western blot analysis or further processed for cyst culture or proliferation assay. Transfection efficiency was monitored using confocal microscopy of transfected cells cultured on chambered glass slides in order to analyse siRNA subcellular localization and stability (data not shown). The molecular target nomenclature for TRPP2 (polycystin-2) conforms to BJP's Concise Guide to PHARMACOLOGY (Alexander *et al.*, 2013).

Western blot analysis

Lysates of control and transfected cells were prepared in RIPA (50 mM Tris-HCl pH 7.4, 150 mM NaCl, 1% Triton X-100, 1% sodium deoxycholate, 0.1% SDS, 1 mM EDTA) with protease inhibitor. Protein fractions (50 μg) were separated on 4–12% Bis-Tris acrylamide gels, transferred to polyvinylidine difluoride membranes and incubated in blocking buffer (LiCor Biosciences, Lincoln, NE, USA) for 2 h and then overnight at 4°C with anti-TRPP2 antibody (Santa Cruz Biotechnology, Inc., Santa Cruz, CA, USA) or mouse monoclonal anti-β-actin (AbCam, Cambridge, UK) in PBS. Blots were washed three times in PBS/0.01% TWEEN 20 then incubated with IR Dye anti-goat/mouse secondary antiserum (1:5000; LiCor Biosciences) for 1 h, each at room temperature. Immunostained proteins were visualized and quantified using an infrared imaging system (Odyssey, LiCor Biosciences).

Data analysis and statistical procedures

Data are presented as mean and SEM from n independent experiments Statistical tests were performed using Prism 5.0.4 (GraphPad Software) as stated in the text.

Chemicals

All materials used in this study were from Sigma Aldrich unless otherwise specified.

Results

Naringenin inhibits growth of Dictyostelium

To identify the molecular mechanism of action of naringenin, we first defined conditions suitable for screening a *Dictyostelium* REMI mutant library. The growth of wild-type *Dictyostelium* in shaking cultures was reduced after 48–96 h by naringenin with an EC_{50} between 50 and 100 μM (Figure 2A). In contrast, development of *Dictyostelium* on nitrocellulose filters (where starved cells aggregate and form fruiting bodies) was unaffected in the presence of up to 200 μM naringenin (data not shown). This growth inhibition enabled the selection of cells resistant to the effect of naringenin in shaking culture using a library of REMI mutants, exposed to 200 μM naringenin for 21 days. Sequence analysis of cells resistant to naringenin under these conditions identified 26 mutants containing an interrupted open reading frame potentially controlling the effect of naringenin on growth (Supporting Information Figure S1). One of these interrupted genes, *pkd2*, encoded the TRPP2 protein (DDB_G0272999). This protein showed a similar overall size (82.2 kDa; 715 aa) to the human protein (variant 1; 87.0 kDa; 758 aa), with similar potential transmembrane domains (Supporting Information Figure S2) although it showed low homology to the human protein (26% identity, 49% similarity; Supporting Information Figure S3).

TRPP2 mediates the effect of naringenin on Dictyostelium

Recapitulation of the gene knockout mutant, *pkd2*$^-$, in wild-type cells (Supporting Information Figure S4) enabled the comparison of the effect of naringenin on wild-type and *pkd2*$^-$ cells. Initial analysis of these two cell lines showed that 100 μM naringenin caused a significant 37% reduction ($P < 0.001$) in wild-type cell growth at 48 and 72 h (Supporting Informatioin Figure S5), whereas the *pkd2*$^-$ mutant showed reduced growth compared with wild-type cells in the absence of naringenin, but showed no significant change in

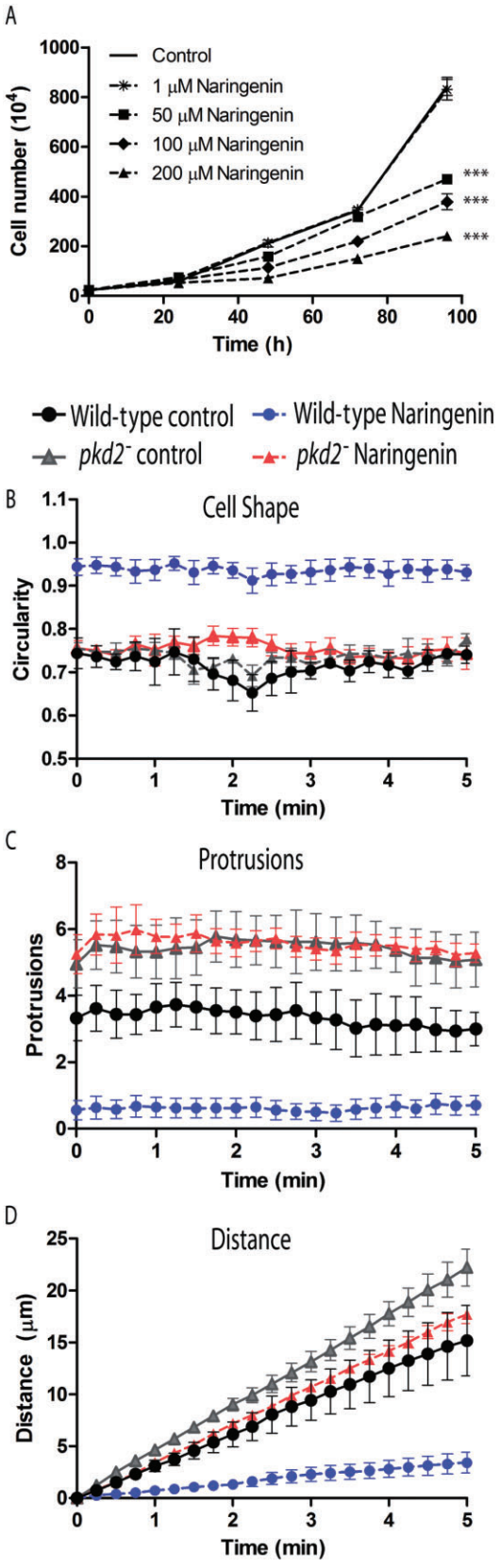

Figure 2

Naringenin reduced growth of *Dictyostelium* and inhibited cell behaviour, an effect controlled through the TRPP2 protein. (A) *Dictyostelium* growth in liquid culture is reduced in a concentration-dependent manner by naringenin. Ablation of the gene encoding TRPP2 showed resistance to the effect of naringenin on cell behaviour, since incubating wild-type and *pkd2*$^-$ cells in 200 μM naringenin (or vehicle control) for 1 h before recording and quantifying cell behaviour over a 5 min period (see Supporting Information Movies S1–S4), showed: (B) Naringenin-treated wild-type cells (blue circles) significantly increased in circularity when compared with vehicle controls (black circles). *pkd2*$^-$ mutant cells did not alter cell shape following naringenin treatment cells. (C) Naringenin-treated wild-type cells (blue circles) significantly decreased pseudopod formation when compared with vehicle controls or *pkd2*$^-$ mutant cells; and (D) Naringenin-treated wild-type cells (blue circles) significantly reduced motility (measured by distance travelled) compared with vehicle controls or *pkd2*$^-$ mutant cells. All data are shown from quadruplicate independent experiments ± SEM.

growth in the presence of 100 μM naringenin at both time points. To better quantify this resistant phenotype, and because we have also shown the effect of a range of dietary compounds on *Dictyostelium* cell behaviour (Robery *et al.*, 2011), we also examined a role for naringenin regulating cell shape and movement. In these experiments, cells were developed under control conditions over a 5 h period, and then treated with 200 μM naringenin for 60 min before recording random cell movement. Naringenin treatment (compare Supporting Information films S1 and S2) caused wild-type cells to round up (Figure 2B; $P < 0.001$ comparing wild-type naringenin, untreated and treated), with a loss of pseudopod formation (Figure 2C; $P < 0.001$ comparing wild-type naringenin, untreated and treated) and a block in cell movement (Figure 2D; $P < 0.01$ comparing wild-type naringenin, untreated and treated). In contrast, the naringenin-treated *pkd2*$^-$ mutant (see Supporting Information films S3 and S4) showed no significant change in shape, measured as roundness (Figure 2B), did not form a significantly different number of pseudopods (Figure 2C), and did not significantly change cell movement (Figure 2D). These data suggest that TRPP2 controls the function of naringenin on *Dictyostelium* movement.

Naringenin inhibits growth of MDCK cells and cysts

As mutations within the human TRPP2 protein are associated with growth of renal cysts in polycystic kidney disease (PKD, Chapin and Caplan, 2010), we next investigated a similar effect of naringenin on the mammalian TRPP2 during cell growth. TRPP2 is expressed in the MDCK canine kidney cell line (Scheffers *et al.*, 2000; 2002) and cyst formation in these cells has been used as a model of PKD (Li *et al.*, 2004; 2012). In this system, naringenin inhibited the growth of MDCK cells over 24–48 h (Figure 3) with EC_{50} values of 28.5 ± 1 μM using two independent assays for cell growth assessment (neutral red assay and SRB).

To investigate the relevance of this mechanism to cyst formation, we then examined the effect of naringenin in regulating the growth of cysts in this cell line over 6 days

(Figure 4). MDCK cells can be induced to form cysts by the addition of forskolin (10 μM) to the growth medium bathing a collagen gel inoculated with the cells. Following this treatment, cysts were observed after 3 days, with individual cysts reaching sizes of >50 μm in diameter 6 days after induction. Addition of naringenin (1–100 μM) caused a concentration-dependent decrease in cyst size, with an EC_{50} of 3–10 μM following a 12 day treatment. Growth inhibition was complete after 6 days exposure to 100 μM naringenin (12 days post-induction); no cysts remained at this concentration. Metformin (10 μM), an activator of AMP-dependent kinase, also inhibited cyst growth, as reported in another study (albeit at 1 mM over 20 days; Takiar *et al.*, 2011).

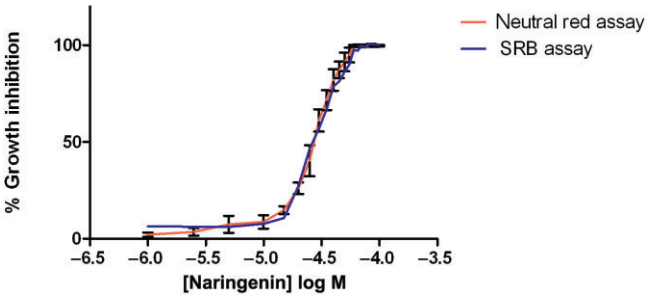

Figure 3

Inhibition of proliferating, unpolarized MDCK cell growth by naringenin after 48 h. Cell viability was measured using the neutral red assay and the SRB protein assay. Data are from three independent experiments showing mean and SEM (error bars not shown for SRB for clarity). EC_{50} values were calculated by non-linear regression (Graph Pad Prism 5). EC_{50} values were 28 ± 1 μM (neutral red assay) and 29 ± 1 μM (SRB assay). R values were >0.98.

Knockdown of TRPP2 (polycystin-2) protects MDCK cysts and cells from naringenin

As it was clear that naringenin inhibited the proliferation of MDCK cells and cysts, we implemented an siRNA strategy to knock down the cellular level of TRPP2 in MDCK cells. In this approach, cell extracts derived from MDCK in isolated cell culture were analysed by Western blot and were positive for TRPP2: two proteins (~90 and ~130 kDa) were detected as shown previously (Wang *et al.*, 2012). Transforming these cells with siRNA specific to TRPP2 RNA or with a scrambled sequence, and leaving cells to recover for up to 48 h, enabled the assessment of reduced MDCK protein by Western blot analysis. This approach gave a dose-dependent decrease in the abundance of both TRPP2 proteins using specific TRPP2 siRNA at 10 nmol (TRPP2 + scrambled siRNA) or 20 nmol (TRPP2 siRNA only; $P < 0.05$ and $P < 0.001$, $n = 5$ respectively). Protein abundance was decreased (compared with untransfected cells) to 56 ± 5% with 20 nmol of TRPP2 siRNA after 24 h, 39 ± 8% after 48 h, and 32 ± 2% after 12 days (Figure 5).

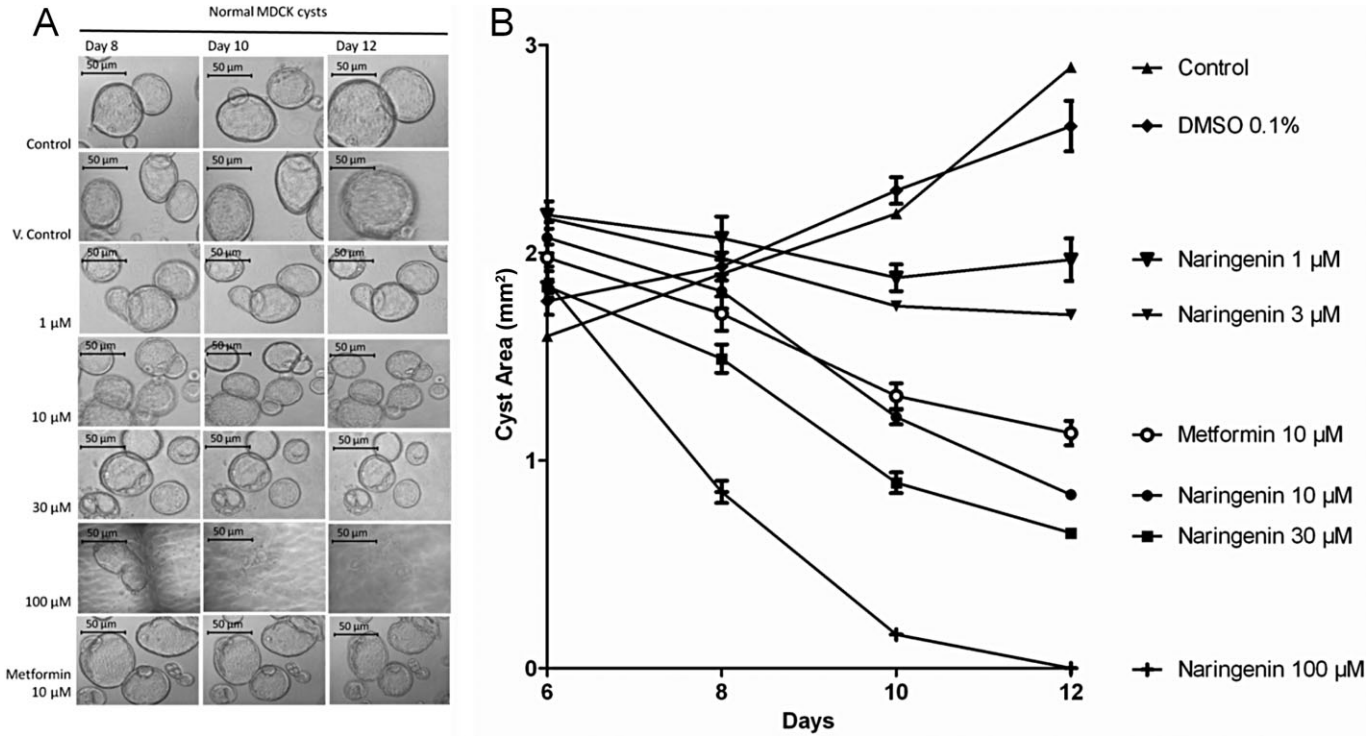

Figure 4

Inhibition of cyst growth by naringenin. (A) Photomicrographs of normal cysts treated from day 6 to day 12 with medium (control), 0.1% DMSO (vehicle control), naringenin 1–100 μM or metformin 10 μM. The shadows/lines in some images are the gridlines used to identify the positions of the cysts. Scale bar is 50 μm. (B) Plot of cyst size versus treatment. Naringenin inhibited cyst growth in a concentration-dependent manner. Metformin (10 μM) inhibited cyst growth as expected. Data are from three independent experiments showing mean and SEM.

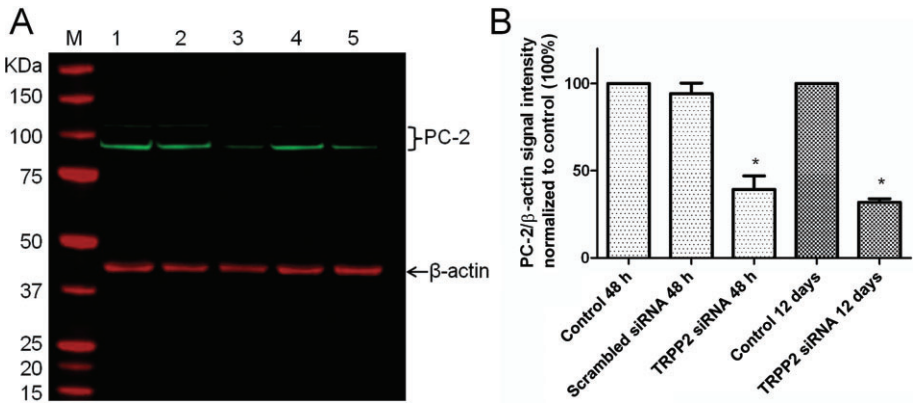

Figure 5

Knockdown of TRPP2 (PC-2) protein in MDCK cells. (A) Representative Western blot of TRPP2 from cells transfected 48 h (lanes 1–3) or 12 days (lanes 4–5). Lane 1: untransfected cells (48 h), Lane 2: cells transfected with scrambled siRNA (48 h), Lane 3: cells transfected with TRPP2 siRNA (48 h), Lane 4: untransfected cells (12 days), Lane 5: cells transfected with TRPP2 siRNA (12 days). M: molecular marker. Sample loading concentration 30 μg per lane. (B) Bands of TRPP2/β-actin fluorescence normalized to untransfected cells. Data are shown as mean ± SEM, $n = 3–5$. *$P > 0.05$ relative to day-matched control.

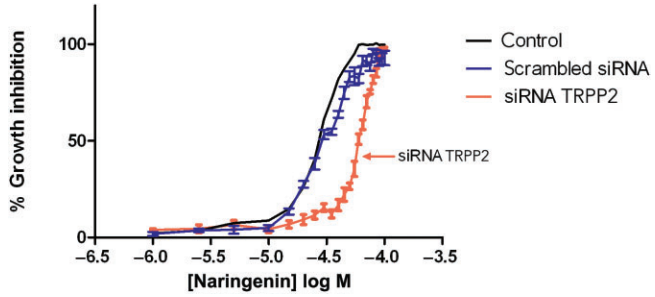

Figure 6

Reduced inhibition of MDCK cell growth transfected with TRPP2 siRNA by naringenin after 48 h. The growth of cells transfected with scrambled siRNA and treated with naringenin was unaffected. Cell viability was measured using the neutral red assay. Data are from three independent experiments showing mean and SEM (error bars not shown for clarity for control, untransfected cells).

The growth of MDCK cells transfected with either scrambled siRNA or TRPP2 siRNA was then measured in the presence of increasing concentrations of naringenin for 48 h. The inhibitory effect of naringenin on growth was reduced in cells transfected with TRPP2 siRNA (Figure 6) when compared with untransfected cells and to cells transfected with scrambled siRNA. The EC_{50} value for naringenin was increased from 28 ± 1 μM (as in Figure 3) to 65 ± 1 μM. Transfection with scrambled siRNA had no effect on the EC_{50} for growth inhibition (30 μM). Thus, at a time point (48 h), when TRPP2 protein was reduced to 39% of control (Figure 5), the effect of naringenin on cell growth was blunted and the EC_{50} value more than doubled.

Untransfected MDCK cells and cells transfected with TRPP2 siRNA, were then grown as cysts for 6 days after which naringenin (1–100 μM) was added for another 6 days (until day 12). Transfected cysts with knocked down TRPP2 were larger (both control and vehicle) than their untransfected counterparts, showing that reduced functional TRPP2 levels promotes cyst formation and growth. Transfected cysts were more resistant than control cysts (Figure 7C) to inhibition by naringenin at 10 μM and 30 μM after 6 days (at day 12). Naringenin at 100 μM progressively reduced cyst growth and cysts were absent at 12 days. Metformin (10 μM) also inhibited the growth of transfected cysts with no difference in activity compared with normal cysts, confirming the selectivity of TRPP2 siRNA treatment (Figure 7B).

Lack of effect of naringenin on chloride secretion in MDCK monolayers

Naringenin has been reported to inhibit chloride secretion (in rat colon) at super-physiological concentrations (EC_{50} > 330 μM; Collins *et al.*, 2011), while others have reported that it stimulates chloride secretion (Yang ZH *et al.*, 2008). A reduction in cAMP-dependent chloride secretion is one method for reducing cyst growth (Li *et al.*, 2004). We therefore performed experiments to determine the effect of naringenin on forskolin-induced chloride secretion measured as I_{SC} (Figure 8). Monolayers were treated on both sides with naringenin (30 μM) or its vehicle (0.1% DMSO) followed by forskolin (20 μM, both sides). Forskolin increased I_{SC} by 10.6 ± 3.1 μA·cm^{-2} (mean ± SEM, $n = 6$) in vehicle-treated monolayers, and by 11.6 ± 3.8 μA·cm^{-2} ($n = 6$) in naringenin-treated monolayers, with no significant difference between the means ($P < 0.05$, one-way ANOVA). Ten minutes after addition of forskolin, I_{SC} remained similar in vehicle-treated monolayers (2.0 ± 0.4 μA·cm^{-2}, $n = 6$) and naringenin-treated monolayers (2.1 ± 0.5 μA·cm^{-2}, $n = 6$, $P < 0.05$, one-way ANOVA). Furosemide, an inhibitor of basolateral chloride uptake, added after the forskolin response began to decline, had little or no effect on I_{SC}, indicating that the stimulation of chloride secretion by forskolin was transient in these cells.

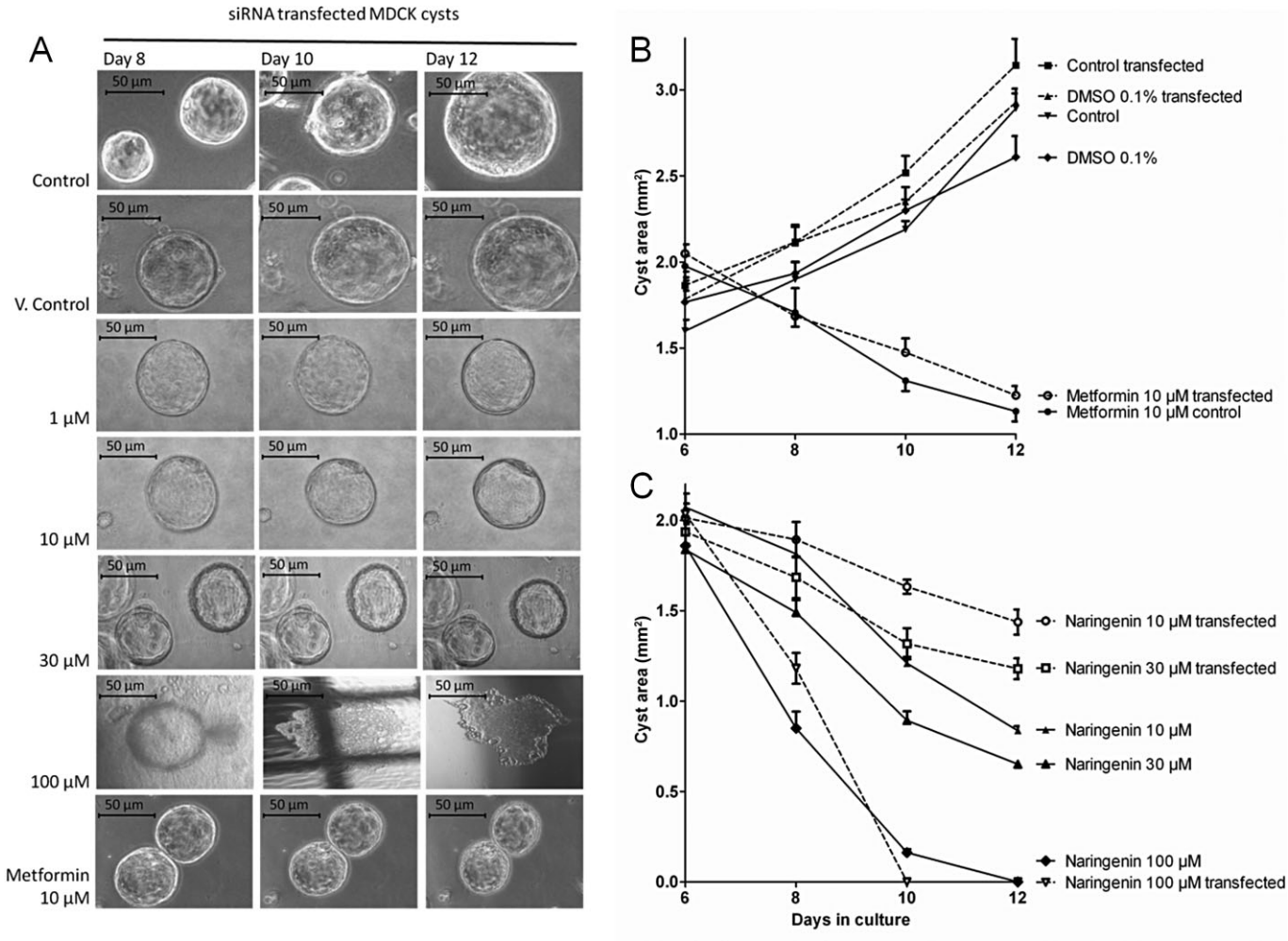

Figure 7

Transfection with siRNA TRPP2 protects cysts from the growth-inhibitory effects of naringenin. (A) Photomicrographs of transfected cysts treated from day 6 to day 12 with medium (control), 0.1% DMSO (vehicle control), naringenin 1–100 μM or metformin 10 μM. The shadows/lines in some images are of the gridlines used to identify the positions of the cysts. Scale bar is 50 μm. (B) Plot of cyst size showing effect of medium (control), DMSO 0.1% (vehicle control) or metformin (10 μM) on control and transfected cysts. (C) Plot of cyst size comparing effect of naringenin in control and transfected cysts. Data are from three independent experiments showing mean and SEM. Data from control cysts are replotted from Figure 4.

Discussion and conclusions

Naringenin inhibits Dictyostelium *growth via TRPP2*

We show for the first time an inhibitory action of naringenin on renal tubule cell growth and cyst formation and demonstrate the involvement of TRPP2 in these processes. The identification of this effect and mechanism came from the use of *Dictyostelium* as a model organism for pharmacogenetics. In our experiments, naringenin inhibited *Dictyostelium* growth with an EC_{50} value of between 50 and 100 μM, higher than the previously reported value of 20 μM (Russ *et al.*, 2006). Naringenin attenuated cell behaviour (shape, pseudopod formation, random cell movement) after 60 min treatment. The inhibitory effect of naringenin was conferred by the expression of the TRPP2 protein, because the *pkd2*$^{-}$ mutant was insensitive to naringenin-dependent reduction in cell behaviour. In another study, other flavonoids (quercitin, chrysin) including the related compound apigenin (4′,5,7-trihydroxyflavone; naringenin is 4′,5,7-trihydroxyflavanone) had no effect on *Dictyostelium* proliferation (Russ *et al.*, 2006), suggesting a degree of structural specificity for naringenin presumably through a TRPP2-dependent effect.

Although a mechanism for how TRPP2 regulates *Dictyostelium* cell behaviour is unclear, a role for calcium signalling in *Dictyostelium* has been reported before (Schlatterer and Malchow, 1993; Unterweger and Schlatterer, 1995; Fache *et al.*, 2005). These studies showed that a decrease in extracellular calcium levels instantly decreased cell speed and induced a loss of cell attachment with the substratum caused by loss of intracellular cell structure (Fache *et al.*, 2005), consistent with our findings of a naringenin-induced alteration of cytoskeletal structure and block of cell behaviour. In addi-

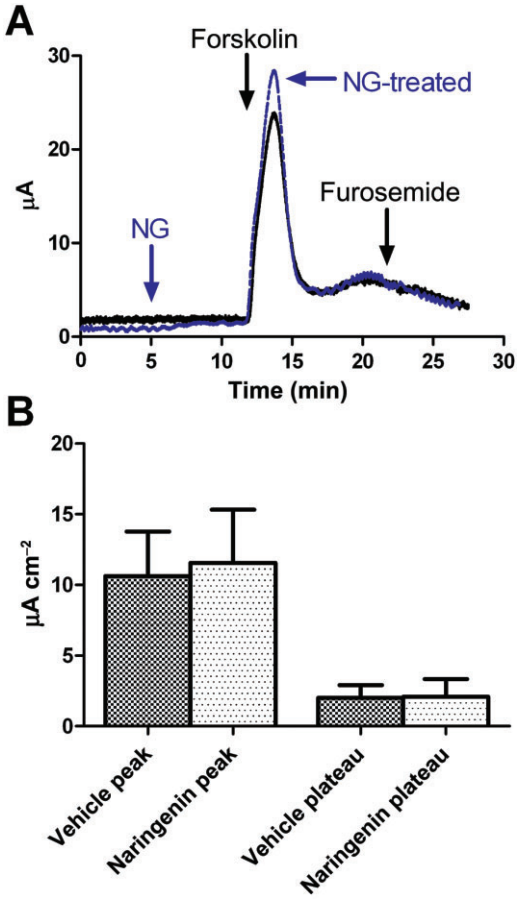

Figure 8

Effect of naringenin on cAMP-dependent chloride secretion. (A) Representative traces showing addition of naringenin (30 µM both sides) or vehicle (DMSO 0.1% both sides), forskolin (20 µM, both sides) and furosemide (100 µM, basolateral) on short-circuit current. (B) Summary data (mean ± SEM, $n = 6$) of effect of naringenin (NG) on forskolin-stimulated responses (peak and plateau, i.e. 10 min after forskolin).

tion, chelating intracellular calcium by loading with BAPTA also prevented cell movement and pseudopod emission (Schlatterer and Malchow, 1993; Unterweger and Schlatterer, 1995). The role of a potential *pkd1* protein (TRPP1) in *Dictyostelium* (DDB_G0289409) can also be considered in future studies.

Naringenin inhibits renal cell growth via TRPP2

Growth of renal MDCK cells and cysts was inhibited by naringenin at similar EC_{50} values (cysts 10 µM, cells 28 µM) to *Dictyostelium* (50 µM). We confirmed that TRPP2 was expressed in MDCK cells and siRNA knockdown of this protein indicated that TRPP2 also regulated the growth-inhibitory action of naringenin in these mammalian cells. Knockdown of TRPP2 in MDCK cells increased resistance to the concentration of naringenin required to reduce cyst growth.

TRPP2 has a number of roles in mammalian cells, and in kidney tubule cells where it is most studied. TRPP2 or polycystin-2 is a member of the TRP family of ion channels, and is a Ca^{2+}-permeable non-selective cation channel (González-Perrett *et al.*, 2001; Menè *et al.*, 2013) located in the endoplasmic reticulum (ER; Koulen *et al.*, 2002) and in the primary cilium (Abdul-Majeed and Nauli, 2011). Shear stress bends the primary cilium and TRPP2 (bound in a complex with TRPP1) admits Ca^{2+} into the cytoplasm. The influx of Ca^{2+} stimulates Ca^{2+} release via TRPP2 on the ER and elevates intracellular Ca^{2+} concentration, with important consequences for growth. Ca^{2+} stimulates PDE and keeps cAMP low, suppressing the Ras/Raf/MEK/ERK pathway of cyst proliferation. When TRPP1 or TRPP2 is disrupted, as in mutations of the corresponding genes PKD1 and PKD2 in PKD, then flow-sensitive Ca^{2+} influx is reduced, cAMP is elevated and the Ras/Raf/MEK/ERK pathway stimulated, leading to cyst proliferation (Abdul-Majeed and Nauli, 2011).

We propose that naringenin may activate TRPP2 to cause Ca^{2+} influx and a decrease in cellular proliferation. Naringenin has been shown to regulate other channels such as the large conductance (BK) K^+ channels in vascular myocytes causing vasorelaxation (Saponara *et al.*, 2006). The possibility that naringenin binds and opens TRPP2, with downstream growth-inhibitory effects, is therefore intriguing and novel.

The TRPP1/TRPP2 complex has other reported effects on growth regulation, and through a diverse range of signalling pathways in addition to Ca^{2+} and cAMP, for example: the mammalian target of rapamycin (mTOR; to decrease cell size and protein synthesis), STAT1/3 (to decrease cell growth and division via p21/cdkc2 inhibition of the cell cycle), G-protein regulated pathways of differentiation, apoptosis and proliferation, and the β-catenin/Wnt pathway for gene expression and differentiation (Chapin and Caplan, 2010). One interesting mechanism is the binding of TRPP2 to the pro-proliferative transcription factor, Id2. In this model of ADPKD genesis, mutations to TRPP2 allow Id2 to enter the nucleus and turn off growth-suppressive genes (Li *et al.*, 2005). A similar mechanism is proposed for TRPP2 in the promotion of phospho-ERK-meditated eIF2α phosphorylation, which down-regulates cell growth (Liang *et al.*, 2008). The role(s) of these pathways in the actions of naringenin requires further investigation.

It is important to note that naringenin was as potent at inhibiting cyst growth as metformin and that the activity of the latter was unaffected by the transfection procedure. Metformin activates AMPK, a kinase that controls growth and metabolism, in part via the actions of mTOR, which is required for growth (Takiar *et al.*, 2011). In addition, AMPK inhibits apical cystic fibrosis transmembrane conductance regulator (CFTR) channels required for Cl^- secretion (Takiar *et al.*, 2011; Li *et al.*, 2012). Metformin therefore inhibits both cystogenesis and chloride secretion and is a potential drug development candidate for ADPKD.

Naringenin does not inhibit Cl^- secretion

Other flavonoids (e.g. genistein and apigenin) modulate CFTR-mediated transepithelial chloride secretion (Li *et al.*, 2004). However, while forskolin stimulated a transient increase in I_{SC} in MDCK cells, in agreement with a previous report (Simmons, 1991), naringenin had no significant effect

on I_{SC} or on the response to forskolin. These data indicate that the reduction in cyst growth was not due to a reduction in cAMP-dependent chloride secretion.

Currently there are no approved clinical therapies for the treatment of PKD (Calvet, 2008; Takiar and Caplan, 2011). Tolvaptan, a vasopressin V_2 receptor antagonist, which is used to reduce cAMP-dependent fluid secretion, reduced the decline in kidney function in patients with ADPKD, but adverse effects led to a high level of discontinuation (Torres *et al*., 2012). Other more experimental strategies include inhibition of CFTR by metformin or direct channel blockers (again to prevent fluid secretion into cysts; Li *et al*., 2004; Yang B *et al*., 2008; Takiar *et al*., 2011); inhibition of mTOR by metformin (Takiar and Caplan, 2011) and inhibition of B-Raf as the crucial point in the MEK/ERK pathway (Calvet, 2008; Takiar and Caplan, 2011). Our results allow us to speculate about a potential use for naringenin in ADPKD treatment. In the minority (15%) of ADPKD patients where TRPP2 function is lost, naringenin would presumably have no effect. In the majority of ADPKD cases, where TRPP1 function is absent (but TRPP2 is present), naringenin could potentially activate TRPP2 to inhibit cyst growth in these patients, providing a novel therapeutic approach for ADPKD treatment. Further study of naringenin as a drug for the treatment of ADPKD is now required.

Acknowledgements

This work was funded by a grant awarded jointly to DB, MAC and RSBW from the SouthWest Academic Network (SWAN), a research collaboration between Kingston University, St George's, and Royal Holloway, University of London. Thanks to Dictybase.org for genome analysis facility. We thank Dr Mark Dockrell, South West Thames Renal Institute, for helpful comments on the original paper. MHRL and SR were funded by PhD studentships from Alzheimer's Research UK and UFAW respectively, both to RSBW. Some of the work for the revised manuscript was performed by AW at his current address, in the laboratory of Dr Rita Jabr and Professor Chris Fry (Department of Biochemistry and Physiology, University of Surrey), to whom we are very grateful.

Conflict of interest

The authors have no conflicts of interest.

References

Abdul-Majeed S, Nauli SM (2011). Calcium-mediated mechanisms of cystic expansion. Biochim Biophys Acta 1812: 1281–1290.

Adachi H, Hasebe T, Yoshinaga K, Ohta T, Sutoh K (1994). Isolation of *Dictyostelium discoideum* cytokinesis mutants by restriction enzyme-mediated integration of the blasticidin S resistance marker. Biochem Biophys Res Commun 205: 1808–1814.

Alexander SPH, Benson HE, Faccenda E, Pawson AJ, Sharman JL, Catterall WA, Spedding M, Peters JA, Harmar AJ and CGTP Collaborators (2013). The Concise Guide to PHARMACOLOGY 2013/14: Overview. Br J Pharmacol 170: 1449–1867.

Calvet JP (2008). Strategies to inhibit cyst formation in ADPKD. Clin J Am Soc Nephrol 3: 1205–1211.

Chang P, Orabi B, Deranieh RM, Dham M, Hoeller O, Shimshoni JA *et al*. (2012). The antiepileptic drug valproic acid and other medium-chain fatty acids acutely reduce phosphoinositide levels independently of inositol in *Dictyostelium*. Dis Model Mech 5: 115–124.

Chapin H, Caplan M (2010). The cell biology of polycystic kidney disease. J Cell Biol 191: 701–710.

Collins D, Kopic S, Geibel JP, Hogan AM, Medani M, Baird AW *et al*. (2011). The flavonone naringenin inhibits chloride secretion in isolated colonic epithelia. Eur J Pharmacol 668: 271–277.

Erlund I, Meririnne E, Alfthan G, Aro A (2001). Plasma kinetics and urinary excretion of the flavanones naringenin and hesperetin in humans after ingestion of orange juice and grapefruit juice. J Nutr 131: 235–241.

Fache S, Dalous J, Engelund M, Hansen C, Chamaraux F, Fourcade B *et al*. (2005). Calcium mobilization stimulates *Dictyostelium discoideum* shear-flow-induced cell motility. J Cell Sci 118: 3445–3457.

González-Perrett S, Kim K, Ibarra C, Damiano AE, Zotta E, Batelli M *et al*. (2001). Polycystin-2, the protein mutated in autosomal dominant polycystic kidney disease (ADPKD), is a Ca^{2+}-permeable nonselective cation channel. Proc Natl Acad Sci USA 98: 1182–1187.

Kale A, Gawande S, Kotwal S (2008). Cancer phytotherapeutics: role for flavonoids at the cellular level. Phytother Res 22: 567–577.

Koulen P, Cai Y, Geng L, Maeda Y, Nishimura S, Witzgall R *et al*. (2002). Polycystin-2 is an intracellular calcium release channel. Nat Cell Biol 4: 191–197.

Kuspa A (2006). Restriction enzyme-mediated integration (REMI) mutagenesis. Methods Mol Biol 346: 201–209.

Leonardi T, Vanamala J, Taddeo SS, Davidson LA, Murphy ME, Patil BS *et al*. (2010). Apigenin and naringenin suppress colon carcinogenesis through the aberrant crypt stage in azoxymethane-treated rats. Exp Biol Med 235: 710–717.

Li H, Findlay IA, Sheppard DN (2004). The relationship between cell proliferation, Cl^- secretion, and renal cyst growth: a study using CFTR inhibitors. Kidney Int 66: 1926–1938.

Li H, Yang W, Mendes F, Amaral MD, Sheppard DN (2012). Impact of the cystic fibrosis mutation F508del-CFTR on renal cyst formation and growth. Am J Physiol Renal Physiol 303: F1176–F1186.

Li X, Luo Y, Starremans PG, McNamara CA, Pei Y, Zhou J (2005). Polycystin-1 and polycystin-2 regulate the cell cycle through the helix-loop-helix inhibitor Id2. Nat Cell Biol 7: 1202–1212.

Liang G, Yang JW, Wang Z, Li Q, Tang Y, Chen X-Z (2008). Polycystin-2 down-regulates cell proliferation via promoting PERK-dependent phosphorylation of eIF2. Hum Mol Genet 17: 3254–3262.

Manach C, Williamson G, Morand C, Scalbert A, Rémésy C (2005). Bioavailability and bioefficacy of polyphenols in humans. I. Review of 97 bioavailability studies. Am J Clin Nutr 81: 230S–242S.

Meiyanto E, Hermawan A, Anindyajati A (2012). Natural products for cancer-targeted therapy: citrus flavonoids as potent chemopreventive agents. Asian Pac J Cancer Prev 13: 427–436.

Menè P, Punzo G, Pirozzi N (2013). TRP channels as therapeutic targets in kidney disease and hypertension. Curr Top Med Chem 13: 386–397.

Moon YJ, Wang X, Morris ME (2006). Dietary flavonoids: effects on xenobiotic and carcinogen metabolism. Toxicol in Vitro 20: 187–210.

Pakes NK, Veltman DM, Rivero F, Nasir J, Insall R, Williams RS (2012). The Rac GEF ZizB regulates development, cell motility and cytokinesis in *Dictyostelium*. J Cell Sci 125: 2457–2465.

Repetto G, del Peso A, Zurita JL (2008). Neutral red uptake assay for the estimation of cell viability/cytotoxicity. Nat Protoc 3: 1125–1131.

Robery S, Mukanowa J, Percie du Sert N, Andrews PL, Williams RS (2011). Investigating the effect of emetic compounds on chemotaxis in *Dictyostelium* identifies a non-sentient model for bitter and hot tastant research. PLoS ONE 6: e24439.

Russ R, Martinez R, Ali H, Steimle PA (2006). Naringenin is a novel inhibitor of *Dictyostelium* cell proliferation and cell migration. Biochem Biophys Res Commun 345: 516–522.

Saponara S, Testai L, Iozzi D, Martinotti E, Martelli A, Chericoni S *et al*. (2006). (+/–)-Naringenin as large conductance Ca^{2+}-activated K^+ (BKCa) channel opener in vascular smooth muscle cells. Br J Pharmacol 149: 1013–1021.

Scheffers MS, van der Bent P, Prins F, Spruit L, Breuning MH, Litvinov SV *et al*. (2000). Polycystin-1, the product of the polycystic kidney disease 1 gene, co-localizes with desmosomes in MDCK cells. Hum Mol Genet 9: 2743–2750.

Scheffers MS, Le H, van der Bent P, Leonhard W, Prins F, Spruit L *et al*. (2002). Distinct subcellular expression of endogenous polycystin-2 in the plasma membrane and Golgi apparatus of MDCK cells. Hum Mol Genet 11: 59–67.

Schlatterer C, Malchow D (1993). Intercellular guanosine-5′-0-(3-thiotriphosphate) blocks chemotactic motility of *Dictyostelium discoideum* amoebae. Cell Motil Cytoskeleton 25: 298–307.

Schneider CA, Rasband WS, Eliceiri KW (2012). NIH Image to ImageJ: 25 years of image analysis. Nat Methods 9: 671–675.

Simmons NL (1991). Chloride secretion stimulated by prostaglandin E1 and by forskolin in a canine renal epithelial cell line. J Physiol 432: 459–472.

Sussman M (1987). Cultivation and synchronous morphogenesis of *Dictyostelium* under controlled experimental conditions. Methods Cell Biol 28: 9–29.

Takiar V, Caplan MJ (2011). Polycystic kidney disease: pathogenesis and potential therapies. Biochim Biophys Acta 1812: 1337–1343.

Takiar V, Nishio S, Seo-Mayer P, King JD Jr, Li H, Zhang L *et al*. (2011). Activating AMP-activated protein kinase (AMPK) slows renal cystogenesis. Proc Natl Acad Sci USA 108: 2462–2467.

Terbach N, Shah R, Kelemen R, Klein PS, Gordienko D, Brown NA *et al*. (2011). Identifying an uptake mechanism for the antiepileptic and bipolar disorder treatment valproic acid using the simple biomedical model *Dictyostelium*. J Cell Sci 124: 2267–2276.

Terryn S, Ho A, Beauwens R, Devuyst O (2011). Fluid transport and cystogenesis in autosomal dominant polycystic kidney disease. Biochim Biophys Acta 1812: 1314–1321.

Torres VE, Chapman AB, Devuyst O, Gansevoort RT, Grantham JJ, Higashihara E *et al*. (2012). Tolvaptan in patients with autosomal dominant polycystic kidney disease. N Engl J Med 367: 2407–2418.

Tyson RA, Epstein DBA, Anderson KI, Bretschneider T (2010). High resolution tracking of cell membrane dynamics in moving cells: an electrifying approach. Math Model Nat Phenom 5: 34–55.

Unterweger N, Schlatterer C (1995). Introduction of calcium buffers into the cytosol of *Dictyostelium discoideum* amoebae alters cell morphology and inhibits chemotaxis. Cell Calcium 17: 97–110.

Vassilev PM, Guo L, Chen XZ, Segal Y, Peng JB, Basora N *et al*. (2001). Polycystin-2 is a novel cation channel implicated in defective intracellular Ca^{2+} homeostasis in polycystic kidney disease. Biochem Biophys Res Commun 282: 341–350.

Wang Q, Dai XQ, Li Q, Wang Z, Cantero MdR, Li LS *et al*. (2012). Structural interaction and functional regulation of polycystin-2 by filamin. PLoS ONE 7: e40448.

Weng CJ, Yen GC (2012). Flavonoids, a ubiquitous dietary phenolic subclass, exert extensive *in vitro* anti-invasive and *in vivo* anti-metastatic activities. Cancer Metastasis Rev 31: 323–351.

Williams RS, Boeckeler K, Gräf R, Müller-Taubenberger A, Li Z, Isberg RR *et al*. (2006). Towards a molecular understanding of human diseases using *Dictyostelium discoideum*. Trends Mol Med 12: 415–424.

Yang B, Sonawane ND, Zhao D, Somlo S, Verkman AS (2008). Small-molecule CFTR inhibitors slow cyst growth in polycystic kidney disease. J Am Soc Nephrol 19: 1300–1310.

Yang ZH, Yu HJ, Pan A, Du JY, Ruan YC, Ko WH *et al*. (2008). Cellular mechanisms underlying the laxative effect of flavonol naringenin on rat constipation model. PLoS ONE 3: e3348.

Supporting information

Additional Supporting Information may be found in the online version of this article at the publisher's web-site:

http://dx.doi.org/10.1111/bph.12443

Figure S1 *Dictyostelium* REMI mutants identified in a growth screen where cells were exposed to naringenin (200 μM) over 21 days. Genes are identified by individual dictybase identifier, gene name (where available) and potential protein functions.

Figure S2 The *Dictyostelium* TRPP2 (polycystein-2) like protein (DDB_G0272999) showed a similar domain structure to the human TRPP2 protein, although it lacked a clearly defined coiled-coil domain.

Figure S3 Alignment of TRPP2 proteins *Dictyostelium* and humans. The *Dictyostelium* TRPP2 protein (DDB_G0272999), human polycystic kidney disease 2-like 1 protein isoform 2 (Hs_TRPP3; NP_001240766) and human polycystic kidney disease type II protein (Hs_TRPP2_V1; AAC16004) were aligned using ClustalW. This alignment shows that the N-terminal region of TRPP2 conserved in animal species and associated with cilial targeting of the protein is not conserved in the *Dictyostelium* protein (Geng L *et al*., 2006). The GSK-3 dependent phosphorylation site S76 (Streets *et al*., 2006), the casine kinase 2 phosphorylation site at S812, responsible for restricting protein localisation to the ER and cilia (Cai *et al*., 2004), and the PKD-dependent phosphorylation site, S801 (Streets *et al*., 2010; all highlighted), are also not conserved in the *Dictyostelium* protein.

Figure S4 The *Dictyostelium pkd2*$^-$ mutant was recapitulated in wild-type cells by the construction of a knockout vector

with the central coding region of the *pkd2* gene replaced by a blasticidin resistance cassette (BsR). Homologous integration of this cassette into wild-type cells and screening by PCR for genomic (G), Vector (V) and knockout (KO) PCR products for the 5′ and 3′ targeting region identified independent *pkd2*-mutants.

Figure S5 Ablation of *Dictyostelium* the *pkd2* gene provides resistance to naringenin during growth. *Dictyostelium* cells grown in still culture over a 72 h period show reduced proliferation in the presence of naringenin (100 μM). Ablation of *pkd2* slows growth in these cells under control conditions, but cells do not show a further reduction in growth in the presence of naringenin (100 μM) suggesting resistance to naringenin during growth.

Movie S1 Wild-type Dictyostelium cell movement. Dictyostelium wild-type (A×2) cells, were induced to chemotax by repeated pulsing with cAMP over a 5 h period, and random cell movement was monitored by time-lapse photography, capturing one image every 15 s for 5 min. Cell behaviour was quantified by computer-generated outlines that are used to calculate average cell shape (circularity), protrusion formation and motility.

Movie S2 Wild-type *Dictyostelium* cell movement following naringenin treatment. *Dictyostelium* wild-type (A×2) cells, were induced to chemotax by repeated pulsing with cAMP over a 5 h period, and then exposed to 200 mM naringenin for 60 min, and random cell movement was monitored by time-lapse photography, capturing one image every 15 s for 5 min. Cell behaviour was quantified by computer-generated outlines that are used to calculate average cell shape (circularity), protrusion formation and motility.

Movie S3 *pkd2-Dictyostelium* cell movement. *Dictyostelium* wild-type (A×2) cells, were induced to chemotax by repeated pulsing with cAMP over a 5 h period, and random cell movement was monitored by time-lapse photography, capturing one image every 15 s for 5 min. Cell behaviour was quantified by computer-generated outlines that are used to calculate average cell shape (circularity), protrusion formation and motility.

Movie S4 *pkd2-Dictyostelium* cell movement following naringenin treatment. *Dictyostelium* wild-type (A×2) cells, were induced to chemotax by repeated pulsing with cAMP over a 5 h period, and then exposed to 200 mM naringenin for 60 min, and random cell movement was monitored by time-lapse photography, capturing one image every 15 s for 5 min. Cell behaviour was quantified by computer-generated outlines that are used to calculate average cell shape (circularity), protrusion formation and motility.